Korean J. Chem. Eng., **27**(4), 1278-1283 (2010)
DOI: 10.1007/s11814-010-0191-x

Behavior of diffusing elements from an integrated cathode of an electrochemical reduction process

Byung Heung Park† and Jin-Mok Hur

Korea Atomic Energy Research Institute, 1045 Daedeokdaero, Yuseong, Daejeon 305-353, Korea
(*Received 19 October 2009 • accepted 24 November 2009*)

Abstract−The electrochemical reduction process for spent oxide fuel is operated in a molten salt bath and adopts an integrated cathode in which the oxides to be reduced act as a reactive cathode in the molten salt electrolyte cell. Heat-generating radioisotopes in the spent oxide fuel such as cesium and strontium are dissolved in the molten salt and diffuse from the integrated cathode. However, the behavior of the dissolved cations has not been clarified under an electrochemical reduction condition. In this work, the reduction potentials of cesium, strontium, and barium were measured in a molten LiCl-3 wt% Li_2O salt and their mass transfer behavior was compared with two current conditions on the cell. The concentration changes of the cations in the molten salt phase were measured and no significant differences on the dissolution behavior were found with respect to the current. However, under a continued current condition, the removal of the high heat-generating elements requires more time than the complete reduction of metal oxide due to the slow rate of diffusion.

Key words: Pyroprocessing, Alkali Metal, Alkaline Earth Metal, Reduction Potential, Diffusion

INTRODUCTION

As a back-end of a nuclear fuel cycle based on a pyroprocess, an electrometallurgical technology for treating irradiated metal fuel was proposed and developed at Argonne National Laboratory (ANL) under the integral fast reactor (IFR) concept [1]. Later, the applicability of the pyroprocess was extended to spent oxide fuels discharged from light water reactors (LWRs) by the institute for the purpose of recycling the oxide spent fuels (SFs) as well as recovering the transuranics (TRUs) [2]. The oxide SFs are stable in a molten salt which is used as an electrolyte in an electrometallurgy process known as an electrorefining, and, thus, they cannot be directly introduced into the developed process for metal fuels. To apply the electrometallurgical technology to the spent oxide fuels, a reduction process for converting the oxides into a metallic form must be connected to the electrorefining process as a head-end process. A conventional metallothermic reduction process in a molten chloride salt was investigated using a reactive lithium metal as a reducing agent, known as a lithium process, and actinide oxides were successfully reduced by reactions with the reactive lithium metal [3-5]. However, in the lithium reduction process, the concentration of Li_2O, a byproduct of the reactions between the metal oxides and the lithium metal, inevitably increases as the reductions proceed. The accumulated Li_2O gradually decreases the reaction rate and it has been shown that there is a concentration limitation of 5.1 wt% for reducing americium dioxide to a metallic form [5].

Recently, the lithium process has been replaced by applying a newly developed electrochemical technology to the reduction process. In the field of electrometallurgy, an electrochemical reduction in a molten salt has been studied to produce various metals of a high purity directly from their metal oxides by electrochemical reactions [6,7]. In the electrochemical reduction process, the metal oxides to be reduced are used as a cathode in a molten salt bath and a de-oxidation takes place by ionization of the oxygen elements from the oxides when an electric current is supplied to a cell, which is known as an electro-deoxidation technology. The advantage of this technology is that a metallic reagent does not need to be introduced, and, as a consequence, the concentration of the oxygen ion in the melt can be maintained at a desired value. The electrochemical metallization (reduction) technology has been successfully adopted to nuclear oxide systems of unirradiated U_3O_8 [8-10], UO_2 [11], and mixed oxide of uranium and plutonium (MOX) [12] in a molten LiCl and the uranium oxide based metal oxide systems were successfully reduced to their corresponding metals. Recently, electrochemical reduction experiments with spent fuel were carried out at the Idaho National Laboratory (INL) and more than 98% reduction yields for uranium were reported [13].

An advanced spent fuel conditioning process (ACP) [14] has been proposed and developed by the Korea Atomic Energy Research Institute (KAERI) for the purpose of reducing the volume, the radiotoxicity and the heat load from the SF of the commercial LWRs by transforming the oxide SFs into metals as well as removing high heat-generating radionuclides. An air-oxidation, an electrolytic reduction, a smelting process, and a waste salt treatment are the componential processes of the ACP. The electrolytic reduction process is considered as a main unit process of the ACP since most of the chemical changes take place in this process. During the electrochemical reduction, oxides of alkali metals (AMs) and alkaline earth metals (AEMs) such as Cs_2O, SrO, and BaO are dissolved into a molten LiCl, and then they are selectively separated from a metal product to be transferred to the smelting process. In SFs, compared with the contents of actinides (Acts), small amounts of fission products (FPs) exist as presented in Fig. 1, which is calculated by ORIGEN

†To whom correspondence should be addressed.
E-mail: bhpark@kaeri.re.kr

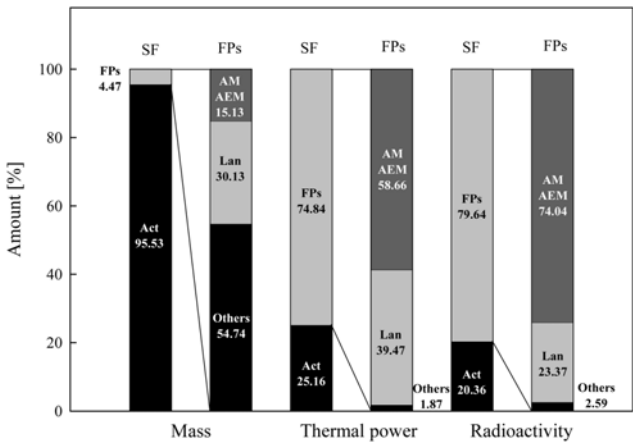

Fig. 1. Mass, thermal power, and radioactivity from a reference SF calculated by ORIGEN 2 code.

2 code based on a 43,000 MWD/MT burnup after a 10-year cooling period. Among the FPs, AMs and AEMs take about 15.13 wt% by mass, but the substantial fractions of thermal power as well as radioactivity coming from them exceed those from lanthanides (Lans) and others. Therefore, the removal of the AMs and AEMs from the SFs would reduce the heat and the radioactivity remaining in metal products after the electrolytic reduction. The dissolution behavior of those oxides from an integrated cathode of the process was investigated in a previous work [15] without applying current. However, under the condition of applying an electric current the behavior has not been studied, so that is the main objective of this work. In the present paper, the reduction potential of dissolved Cs_2O, SrO and BaO was examined and the mass transfer of metal ions was measured in order to clarify the behavior of Cs_2O, SrO, and BaO in the electrolytic reduction process.

ELECTROLYTIC REDUCTION AND REACTIONS OF AM AND AEM OXIDES

Reactions of metal oxides in SFs with LiCl are summarized in Table 1 and reaction Gibbs energies at 650 °C are also presented for each reaction [16]. The AM and AEM oxides in an oxide SF readily react with lithium chloride and transform into their chlorides, while actinide and lanthanide oxides are stable in their oxide forms.

Table 1. Reactions of selected metal oxides with LiCl and reaction Gibbs energy changes at 650 °C

Reaction	ΔG_r^o (kJ/mol O)
$UO_2+4LiCl \rightarrow UCl_4+2Li_2O$	275.538
$PuO_2+4LiCl \rightarrow PuCl_4+2Li_2O$	283.672
$Am_2O_3+6LiCl \rightarrow 2AmCl_3+3Li_2O$	161.300
$Y_2O_3+6LiCl \rightarrow 2YCl_3+3Li_2O$	214.297
$Nd_2O_3+6LiCl \rightarrow 2NdCl_3+3Li_2O$	161.325
$Ce_2O_3+6LiCl \rightarrow 2CeCl_3+3Li_2O$	154.574
$Cs_2O+2LiCl \rightarrow 2CsCl+Li_2O$	−287.571
$SrO+2LiCl \rightarrow SrCl_2+Li_2O$	1.517
$BaO+2LiCl \rightarrow BaCl_2+Li_2O$	−55.538

Cesium, strontium, and barium take most of the amount of AM and AEM in an SF and they are selected as the reference elements of this work.

Interestingly, the reaction Gibbs energy change of the SrO reaction is positive, as listed in Table 1, and an equilibrium constant ($K_{eq}=\exp(-\Delta G_r^o)/RT$) at a standard state is evaluated as 0.82. This indicates that some $SrCl_2$ can be produced under a standard condition even though the reaction Gibbs energy is positive. Moreover, when the amount of LiCl is much larger than SrO as with the process of an electro-chemical reduction, where a ratio of LiCl to SrO is more than a thousand, the reaction with LiCl would transform most of the SrO in a system into $SrCl_2$. Therefore, we can expect that SrO in an SF will completely dissolve in the molten LiCl and exist as a chloride form because the weight fraction of Sr in a SF is less than 0.1% and a weight ratio of $LiCl/U_3O_8$ for the electrolytic reduction is over five [9]. The solubility of $SrCl_2$ in a pure molten LiCl at 650 °C can be found as about 66 mol% from a binary phase diagram [17] and the solubility of Li_2O has been reported as 11.9 mol% [18]. Those solubility data enable us to expect that all the produced $SrCl_2$ and Li_2O would be dissolved in a molten LiCl during the electrochemical reduction process.

The electrolytic reduction takes place by an electrochemical reaction followed by a chemical reaction. On a cathode, lithium metals are electro-chemically produced from their ions and, then, the lithium metals react with metal oxides to be reduced as follows, resulting in a removal of oxygen from the metal oxides:

Cathode:

$$Li^+ + e^- \rightarrow Li \quad (1)$$

$$2yLi + M_xO_y \rightarrow yLi_2O + xM \quad (2)$$

$$Li_2O \rightarrow 2Li^+ + O^{2-} \quad (3)$$

Anode:

$$O^{2-} \rightarrow 1/2O_2 + 2e^- \quad (4)$$

The byproduct, Li_2O, dissolves into a molten salt and dissociates as ions (Eq. (3)). The oxygen anions, finally, transfer to the anode and are oxidized into gases leaving the electrochemical cell as Eq. (4).

AMs and AEMs should be removed from an SF during the electrolytic reduction process to reduce heat load in the metal product. As aforementioned, chlorinated AMs and AEMs are readily dissolved into a molten salt to exist as cations (AM^+ and AEM^{2+}). Therefore, the produced Cs^+, Sr^{2+}, and Ba^{2+} ions will compete with Li^+ at a cathode under an electro-chemically reducing condition as with Li^+ in Eq. (1). The participation of each cation in the electrochemical reduction fully depends on an applied potential. Reduction of metal ions subject to the potential can be compared by the decom-

Table 2. Decomposition potentials at standard state and at 650 °C

Reaction	E(V)
$CsCl \rightarrow Cs+0.5Cl_2$	3.66
$SrCl_2 \rightarrow Sr+Cl_2$	3.58
$BaCl_2 \rightarrow Ba+Cl_2$	3.68
$LiCl \rightarrow Li+0.5Cl_2$	3.46
$Li_2O \rightarrow 2Li+0.5O_2$	2.47

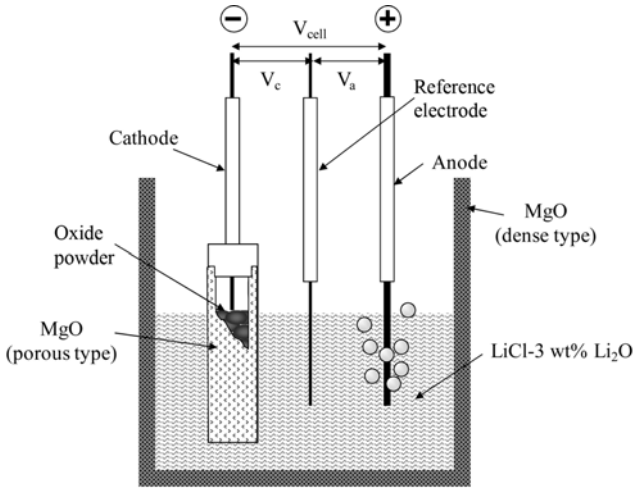

Fig. 2. Schematic description of an electrochemical reduction cell.

position potentials of candidate elements. Table 2 summarizes the cell potential and it suggests that no other cations except for Li^+ will be reduced when the cell potential is controlled between 2.47 and 3.58, where Cs, Sr, and Ba are stable in their ionic forms.

EXPERIMENTAL

The experiments were performed with the apparatus as shown in Fig. 2, which is the same apparatus used in a previous work [14] except that two one-end platinum tubes were inserted in the melt as anodes and a platinum rod was used as a reference electrode. The size of the porous magnesia basket containing solid metal oxide in a powder form is 16 mm in diameter, 2.5 mm in thickness, and 80 mm in length, which is available for up to 5 g/batch scale electrochemical experiments. An inner magnesia crucible, adopted as a melting pot, is a high-density type and its inside diameter is 70 mm. An integrated cathode assembly is devised to load metal oxides to be reduced, where a stainless steel rod is inserted in the middle of stacked powder oxide as a current feeder. The cathode is composed of a ceramic basket, a current feeder and metal oxide to be reduced and its characteristics for the electrolytic reduction of uranium oxide were studied by Park et al. [19]. Two platinum anodes of 6 mm in diameter and 1 mm in thickness are placed for the cathode to be the center between the two anodes, and a platinum rod of 3 mm in diameter was adopted as a quasi-reference electrode to measure each electrode potential following the studies for an electrolytic reduction [8-10,19]. Analytical grade chemicals except for the uranium oxide were used as purchased without any further treatment. The details on the chemical compounds and preparation of the metal oxide mixtures are described in a previous work [15].

The electrodes and a thermocouple were inserted through a reactor flange and then they were fixed at 5 mm above the bottom of the reactor. The lithium chloride was poured into the reactor and the atmosphere was changed into an inert Ar in a gas-tight cell; the atmosphere was further controlled during heating by a purging of Ar gas at a room temperature, 300, and 650 °C. The Li_2O was added after the salt had completely fused and the concentration was confirmed by titration of a salt sample taken at 2 hr after the addition. The WMPG 1000 Multichannel Potentiostat/Galvanostat from WonA-Tech Co. was used for the current/voltage supplier and monitor. By using the WMPG 1000 Ver.3.00 software, the current-voltage was controlled and data were acquired into a PC. Samples were taken from the melt and the metal elements were analyzed by an atomic adsorption spectrophotometer (AAS) and an induced coupled plasma spectrophotometer (ICP).

RESULTS AND DISCUSSION

1. Cyclic Voltammetry (CV)

Cyclic voltammetry (CV) is a useful electro-chemical method to determine the reduction-oxidation behavior of reactive elements in an electrolyte, and a reduction potential can be measured by this method. CV runs started from an open circuit potential (OCP) to a vertex potential of −2.5 V (vs. Pt) and a scanning direction was reversed to complete at 0 V for open cycles or, then, reversed again to −1.0 V presenting closed cycles. In this work, cyclic voltammograms are arranged to be seen in a clockwise direction and potentials are reported versus a Pt reference electrode unless otherwise specified. In general, the reduction potential is measured under a standard condition where the activity of a metal-metal ion couple is unity. However, the present system is associated with a reactive cathode which contains nonconductive metal oxide powder in a nonconductive ceramic basket, and, thus, the polarization response on the working electrode (cathode) is not so fast. Therefore, prior to the CV runs, the scanning rate and the steadiness of the quasi-reference electrode were investigated for a $BaO\text{-}U_3O_8$ loaded cathode (0.5 g BaO+5 g U_3O_8) in a molten LiCl-3 wt% Li_2O salt (125 g LiCl+3.87 g Li_2O).

Resultant CV diagrams with respect to a scanning rate presented in Fig. 3 show that the current is in proportion with the scanning rate, as CV experiments usually exhibit in an electrolyte cell. The increase of current from OCP at scanning rates greater than 10 mV/s may be due to impurities carried by a porous magnesia basket. Porous magnesia baskets had been dried at 100 °C for 10 hrs, but some impurities such as moisture might have remained in the basket pores. The initial current was the lowest at the 10 mV/s scanning

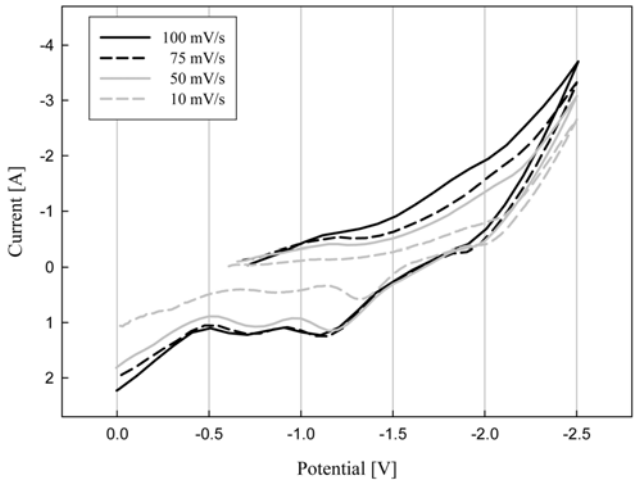

Fig. 3. CV diagrams for a $BaO\text{-}U_3O_8$ loaded cathode with respect to a scanning rate.

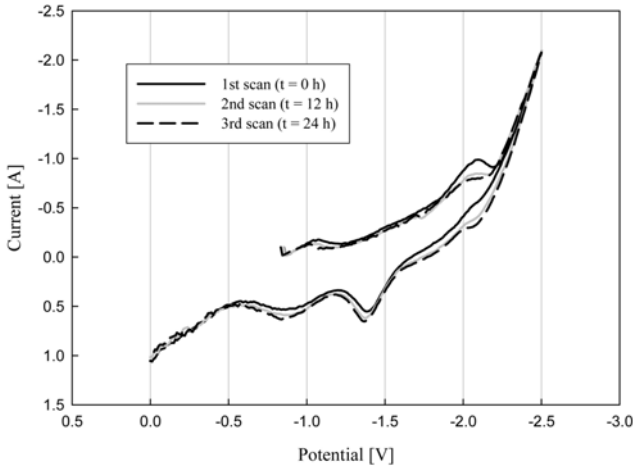

Fig. 4. Reproduced CV diagrams for a BaO-U_3O_8 loaded cathode with a 12-hr time interval.

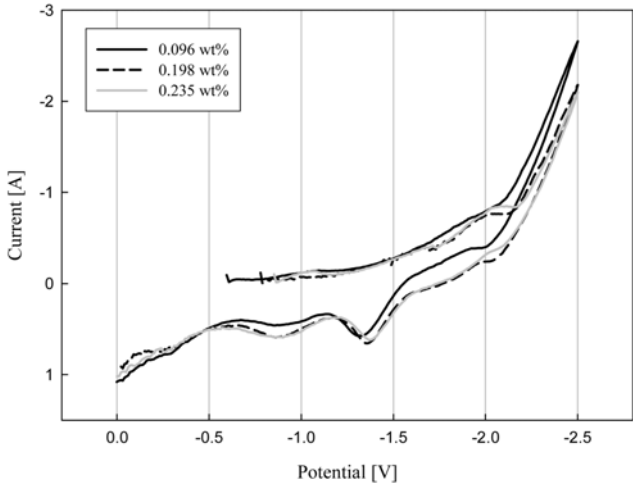

Fig. 5. CV diagrams for a BaO-U_3O_8 loaded cathode with respect to a Ba concentration in a molten salt.

rate, and it was appropriate to identify characteristic waves for the present electrochemical cell. After fixing the scanning rate at 10 mV/s, a fresh cathode of the same type (0.5 g BaO+5 g U_3O_8) was repeatedly scanned three times with a 12-hour interval; the reproduced CV behavior was obtained as shown in Fig. 4, ensuring the applicability and the steadiness of Pt as a quasi-reference electrode. Pt was used as a quasi-reference electrode in this work, which is often employed for a nonaqueous solvent. A Pt reference electrode had been satisfactorily adopted for measuring electrochemical potentials in another molten salt system of Lloyd and Gilbert [20]. The potential in their work revealed a sufficient stability during their experiments and they reported potentials with respect to a Pt reference electrode. Therefore, the stability of a Pt reference electrode in a molten salt at a high temperature has already been proven. BaO loaded with U_3O_8 in a cathode is gradually dissolved into a molten salt phase to accumulate in a bulk phase. The effect of the increased concentration of Ba in the melt on the reduction potential was examined by CV runs at 10 mV/s scanning rate and it presented no remarkable differences within a range of 0.1 to 0.24 wt% as shown in Fig. 5.

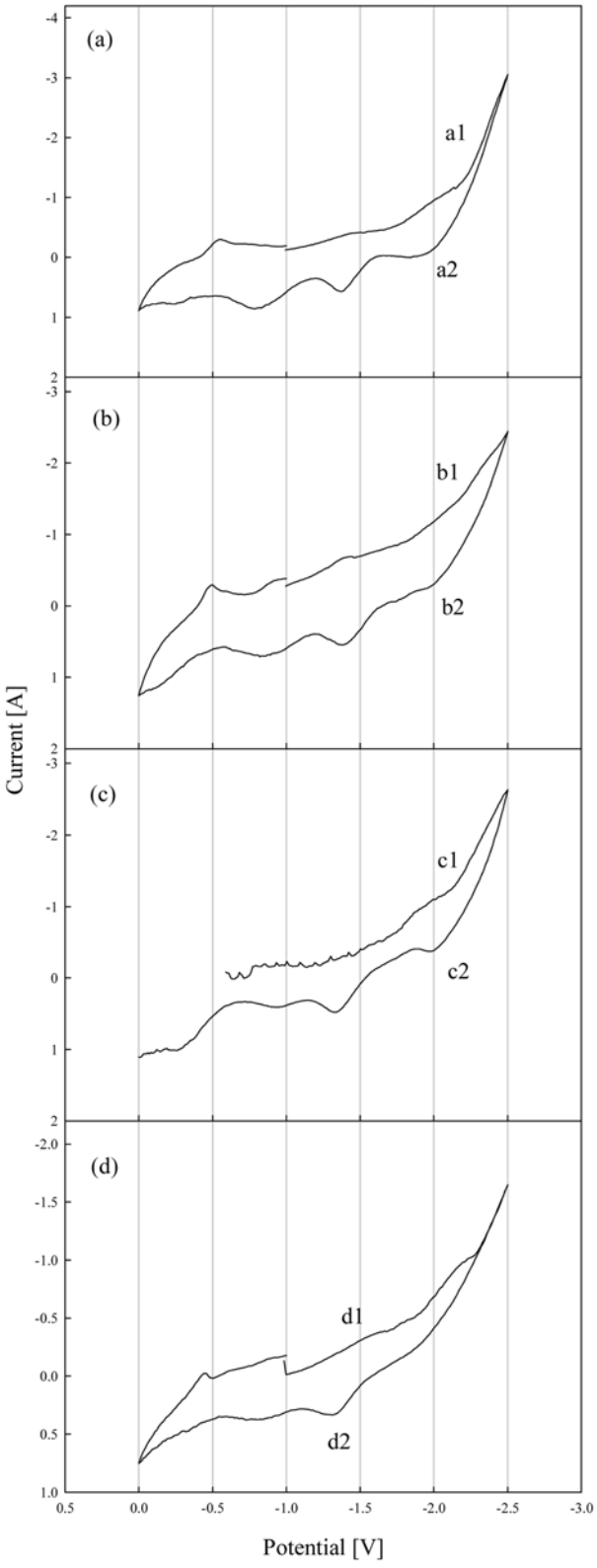

Fig. 6. CV diagrams for (a) Cs_2O-U_3O_8, (b) SrO-U_3O_8, (c) BaO-U_3O_8, and (d) U_3O_8 loaded cathode in a molten LiCl-Li_2O salt.

A CV run was performed for a mixed-oxide loaded cathode with respect to the oxide mixture systems (0.5 g Cs_2O, SrO or BaO+5 g U_3O_8) in a molten LiCl-3 wt% Li_2O salt to identify reduction poten-

tials of cations under a considered condition. Closed CV runs for a Cs_2O-U_3O_8 and a SrO-U_3O_8 system and an open run for a BaO-U_3O_8 system show similar behavior as presented in Fig. 6. The characteristics of the CV diagrams are compared with that from a pure U_3O_8 CV run of Fig. 6(d). A cathode in this system consisted of a metallic current feeder, metal oxide mixture in powder form, and a porous nonconductive magnesia basket. Therefore, ions should pass through two composite porous regions (the metal oxide powder and the porous basket) to respond on an imposed potential. In addition to the physical barrier, the multivalent characteristics of uranium in U_3O_8 were other reasons for the cyclic voltammograms to be seen as Fig. 6; U_3O_8 could be reduced to U_4O_9, UO_2 and metallic uranium by applied potential, and lithium uranates in a form of $Li_xU_yO_z$ could be formed in a molten LiCl-Li_2O salt [21]. Details on the CV behavior of pure U_3O_8 electrochemical reduction in a molten LiCl-Li_2O salt such as Fig. 6(d) were explained by Park et al. [21]. Here, this research focused on analyzing the effect of AM and AEM oxides blended with U_3O_8 powder in a cathode basket on CV responses. Reductive waves found near −2.0 V, which are denoted as a1, b1, and c1 in Fig. 6(a), (b), and (c), respectively, are supposed to be the potentials where Cs^+, Sr^{2+}, and Ba^{2+} are reduced, and a2, b2, and c2 in Fig. 6 might be their corresponding oxidation waves since, at that potential, any distinctive wave was not observed in the U_3O_8 CV run (Fig. 6(d)). The reduction and oxidation waves at around −1.4 V (denoted as d1 and d2 in Fig. 6(d), respectively) which commonly appeared in Figs. 6(a) to (d) are supposed to be the behavior of Li oxidation to Li^+ [21]. In Fig. 6(d), there was a reduction wave at around −1.8 V, but any distinctive corresponding oxidation wave was not found, which means the reduction was irreversible. This behavior is understood as a result of an irreversible reaction between the reduced Li metal and the uranium oxide in the integrated cathode as Eq. (2). Based on the CV experiments, it can be concluded that the reduction potentials of Cs^+, Sr^{2+}, and Ba^{2+} are more cathodic than that of Li^+ as compared in Table 2 for their chloride decomposition potentials.

2. Chronopotentiometry (CP)

The metal ions would diffuse only by concentration differences between the cathode inside and the bulk salt when a cell is free of potential. However, the dissolved Cs^+, Sr^{2+}, and Ba^{2+} ions possess positive charges, which means they would prefer to stay around a cathode during the electrolytic reduction runs under an applied potential field. Therefore, their diffusing behaviors might be different according to the imposed potential. In this work, the dissolution and diffusion of Cs, Sr, and Ba were investigated under an electrolytic reduction condition and compared with the potential-free condition to assess the influence of the potential on the diffusing behavior.

The experimental procedures were exactly the same with the previous work [15] except that a constant current was applied for electrochemical reduction runs because an electrolytic reduction is performed under a constant current condition [8-10]. Experimental conditions of current conditions and initial compositions in a cathode basket are summarized in Table 3. For comparison, the same amount of oxide mixtures of Cs_2O, SrO, or BaO with U_3O_8 were used as a cathode under a current-free and an imposed current condition. The potential behavior of a pure 5 g U_3O_8 reduction run is compared with that of a U_3O_8-Cs_2O reduction run (CS-1) as illustrated in Fig. 7. Under the same current condition of 0.4 A, the two cathodes exhibited

Table 3. Current conditions and initial compositions in a cathode basket

Id.	Current [A]	Chemical	Amount [g]
CS-0	0	U_3O_8	5
CS-1	0.4	Cs_2O	0.5
SR-0	0	U_3O_8	5
SR-1	0.05	SrO	0.1
BA-0	0	U_3O_8	5
BA-1	0.05	BaO	0.1

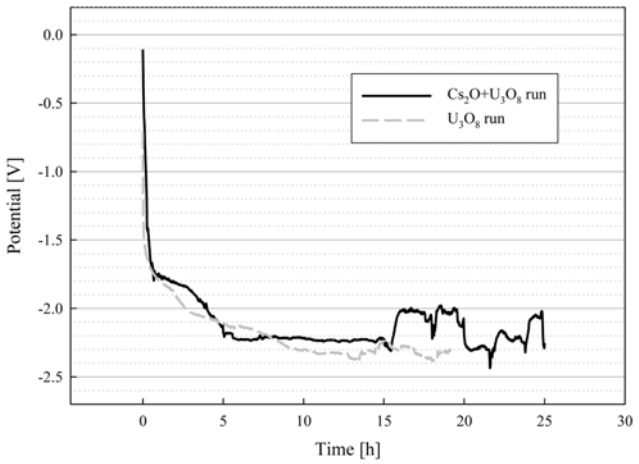

Fig. 7. Chronopotentiograms for a Cs_2O-U_3O_8, and a U_3O_8 runs at 0.4 A.

Table 4. Reactions of Cs, Sr, and Ba with LiCl and U_3O_8 and reaction Gibbs energy changes at 650 °C

Reaction	ΔG_r^o (KJ)
$4Cs+U_3O_8 \rightarrow 2Cs_2O+3UO_2$	−267.884
$Cs+LiCl \rightarrow CsCl+Li$	−19.388
$8Sr+U_3O_8 \rightarrow 8SrO+3U$	−1038.561
$Sr+2LiCl \rightarrow SrCl_2+2Li$	−22.587
$8Ba+U_3O_8 \rightarrow 8BaO+3U$	−747.678
$Ba+2LiCl \rightarrow BaCl_2+2Li$	−43.282

similar responses with time as they are stabilized at around −2.1 V after a transient state. The stable potential of CS-1 run did not exceed the reduction potential of Cs^+ measured in the CV run. If Cs^+, Sr^{2+}, or Ba^{2+} are reduced as their corresponding metals during an electrolytic reduction, it is expected that they would react with U_3O_8 or LiCl as reductants based on the free energy changes [16] at a system temperature as given in Table 4.

Fig. 8 compares the diffusion behavior of metal elements under constant currents with the results from the current-free runs measured in the bulk phase with respect to the experimental time. It also shows no meaningful reduction on the accumulation of the metal elements in the melt by the applied current though the initial concentrations were measured lower than those in the no current conditions. The experimental time was recorded after the Li_2O dissolution completed. The Li_2O in a powder form was added when pure

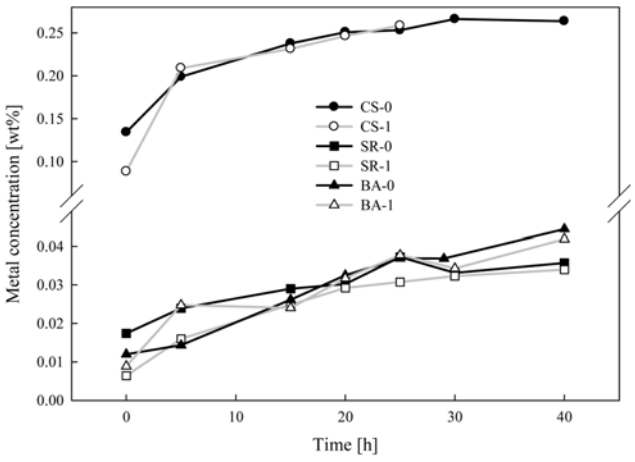

Fig. 8. Concentration changes of metal elements in a molten salt.

LiCl fused and the dissolution took 2 hours, from then current was supplied and the time measured. The metal oxide loaded in the cathode basket went through the melting of LiCl and the dissolution of Li_2O and a portion of the loaded oxide was dissolved during that period. Therefore, the initial concentrations in Fig. 8 were not zeros. As presented in Fig. 8, at low initial concentrations, the linearity of the metal element concentrations was increased and the diffusion rate was decreased. The experimental time for the electrolytic reduction was determined based on the reduction of the loaded U_3O_8; thus, Fig. 8 brought insight that the diffusion of Cs, Sr, and Ba would continue even after the electrochemical runs. Therefore, it can be concluded that the cathode should be immersed in the molten salt bath for a while to increase the removal of Cs, Sr, and Ba from it after the reduction.

CONCLUSIONS

In the electrolytic reduction process where SFs of an oxide form are changed into a metallic form, alkali and alkaline-earth metal oxides dissolve in a molten salt medium. The components of an SF are trapped in a porous magnesia filter which is used as a cathode of the process. Soluble metal oxides diffuse through the pores of the filter and the behavior of this dissolution is investigated in this work.

Cesium, strontium, and barium formed cations when their oxides were dissociated in the molten salt. The reduction potentials of the cations was measured by CV method, and it was found that they would be reduced at more cathodic potential than the reduction of Li^+ in a molten LiCl-3 wt% Li_2O salt. Moreover, the diffusion of the positive-charged species was not affected by the current imposed on the cell when the applied potential on a cathode was controlled not to reduce the metal ions. Therefore, we can conclude that the electrolytic reduction process is very effective for reducing uranium and transuranics to their metallic form and for removing high-heat generating elements such as cesium, strontium, and barium from the metal product to be recovered. However, the rate of diffusion was relatively slow compared with the reduction of uranium under a constant current condition. It suggests that there should be the stay-over of a cathode in a molten salt bath after the reduction.

ACKNOWLEDGEMENT

The R&D described in this paper was supported by Nuclear Research & Development Program of the Korea Science and Engineering Foundation (KOSEF) grant funded by the Korean government (MEST) (Grant code: M20703030001-08M0303-00110).

REFERENCES

1. Y. I. Chang, *Nucl. Technol.*, **88**, 129 (1989).
2. C. C. McPheeters, R. D. Pierce and T. P. Mulcahey, *Progress Nucl. Energy*, **31**, 175 (1997).
3. E. J. Karell, R. D. Pierce and T. P. Mulcahey, *Treatment of oxide spent fuel using the lithium reduction*, ANL Report, ANL/CMT/CP-89562, Argonne National Laboratory, Argonne, U.S.A. (1996).
4. T. Usami, M. Kurata, T. Inoue, H. E. Sims, S. A. Beetham and J. A. Jenkins, *J. Nucl. Mater.*, **300**, 15 (2002).
5. T. Usami, T. Kato, M. Kurata, T. Inoue, H. E. Sims, S. A. Beetham and J. A. Jenkins, *J. Nucl. Mater.*, **304**, 50 (2002).
6. G. Z. Chen, D. J. Fray and T. W. Farthing, *Nature*, **407**, 361 (2000).
7. D. J. Fray, *J. Metals*, **53**, 26 (2001).
8. J.-M. Hur, C.-S. Seo, S.-S. Hong, D.-S. Kang and S. W. Park, *React. Kinet. Catal. Lett.*, **80**, 217 (2003).
9. S. M. Jeong, S.-B. Park, S.-S. Hong, C.-S. Seo and S.-W. Park, *J. Radioanal. Nucl. Chem.*, **268**, 349 (2006).
10. C. S. Seo, S. B. Park, B. H. Park, K. J. Jung, S. W. Park and S. H. Kim, *J. Nucl. Sci. Technol.*, **43**, 587 (2006).
11. K. Gourishankar, L. Redey and M. Williamson, *Electrolytic reduction of metal oxides in molten salts*, Light Metals 2002 (2002).
12. M. Kurata, T. Inoue, J. Serp, M. Ougier and J. P. Glatz, *J. Nucl. Mater.*, **328**, 97 (2004).
13. S. Herrmann, S. Li and M. Simpson, *J. Nucl. Sci. Technol.*, **44**, 361 (2007).
14. S. W. Park, H. S. Park, C. S. Seo, J. M. Hur and Y. S. Hwang, Proc. 3rd Korea-China Joint Workshop on Management of Nuclear Wastes, Shanghai, China (2002).
15. B. H. Park, S. B. Park, S.-H. Choi and C. S. Seo, *J. Chem. Eng. Jpn.*, **39**, 609 (2006).
16. HSC Chemistry®, Outotec Research, 2006, Version 6.0.
17. R. S. Roth, J. R. Dennis and H. F. McMurdie, *Phase diagrams for ceramists*, The American Ceramic Society (1969).
18. G. K. Johnson, R. D. Pierce, D. S. Poa and C. C. McPheeters, in: Mishar B., Averill W. A. Ed., Actinide Processing: Methods and Materials, The Minerals, Metals and Materials Society, TMS, Warrendale, Pennsylvania (1994).
19. S. B. Park, B. H. Park, S. M. Jeong, J. M. Hur, C.-S. Seo, S.-H. Choi and S. W. Park, *J. Radioanal. Nucl. Chem.*, **268**, 489 (2006).
20. C. L. Lloyd and J. B. Gilbert, *J. Electrochem. Soc.*, **141**, 2642 (1994).
21. B. H. Park, I. W. Lee and C.-S. Seo, *Chem. Eng. Sci.*, **63**, 3485 (2008).